The Nucleus ***53****, No. 2 (2016) 107-113*

www.thenucleuspak.org.pk

The Nucleus

ISSN 0029-5698 (Print)

ISSN 2306-6539 (Online)

Computing the Low Dimension Manifold in Dissipative Dynamical Systems

M. Shahzad[1*], F. Sultan[1], I. Haq[1], H.A. Wahab[1], M. Naeem[2] and F. Haq[1]

[1]*Department of Mathematics, Hazara University, Mansehra, Pakistan*

[2]*Department of Information Technology, Abbottabad University of Science and Technology, Abbotabad, Pakistan*

[*]*shahzadmaths@hu.edu.pk; faisalsultan222@gmail.com, ibrarulhaqhu@gmail.com, wahabmaths@hu.edu.pk, mohammadnaeem@gmail.com, fazalhaqphd@gmail.com*

ARTICLE INFO

Article history :
Received : 02 September, 2015
Revised : 25 April, 2016
Accepted : 02 May, 2016

Keywords :
Chemical Combustion
Kinetics Process
Entropy
Refinement
Invariant Manifold
Invariant Grids

ABSTRACT

The importance of the model reduction techniques cannot be denied or ignored for a number of combustion problems in chemical sciences. We examine an analysis of very well-known method by Mass and Pope by measuring the influence of physical processes on the water-gas shift reaction (WGSR). We observe that if the process of physical and chemical reactions is coupled, this will lead to a very dramatic effect. An adaptive parameterization technique is developed for the numerical implementation. Through proper algorithm and grid size variations, the approximate solution is obtained and further refined with the method of invariant grids. Consequently, it leads us to a vicious effect on CPU when we extended this idea to higher dimensions.

1. Introduction

The behaviour of the chemical species (c_i), which are involved in a complex chemical reaction, can easily be monitored if we are capable of transforming the mentioned chemical model into a mathematical model. This will not only help in controlling the system but also enables us to measure the relation among these chemical species.

If a mathematical model involves a linear system, it can easily be handled analytically, but usually, it does not happen. Therefore, we continue with the process numerically with the assumption of small time interval δt replacing the infinitesimal dt for measuring concentration during the next time interval. In this way, we can deduce that stiffness usually arises in the governing equations of chemical reactions.

Now for the construction of slow invariant manifold (SIM), we first need an initial approximation. This initial approximation can be obtained by using any of the newly developed methods [1-5].

Also, there exist such methods [3-7] which automatically calculate the steady state and quasi-equilibrium estimates over all possible thermochemical states of the system by using the fact that during the reaction process, a large number of chemical species move so fast that they can only be decoupled to control or limit the process. Then these decoupled n_f fast reactions may be ignored (as they are faster than the flow-time scale) while the slow ones (progress variables) can be tracked. Based on the same aspects, ILDM method categorizes attracting intrinsic low-dimensional manifolds in $n_s = n - n_f$ dimensional state space (where n implies overall species) with the assumption that after a short time, the thermodynamic state of the system would slow down into the low-dimensional manifold n_s. As the progress variables n_s are responsible for the whole mechanism, we only calculate this variable. This leads to an efficient reduction in CPU time by reducing the complexity of the reaction.

This method is explained with examples in the next sections. For simplification of our problem, we first consider its one-dimensional geometry. The governing equations for the calculation of initial approximations are standard and they can easily be found in many kinds of literature [8-10]. In order to achieve the convergences, these equations are solved in time scale. The idea is then extended to higher dimensions.

[*] Corresponding author

2. Chemical Model

For a basic notation of the chemical kinetics and its formalism, consider a list of the finite set of components with symbols $C_{sp_1},\ldots,C_{sp_n}$ (chemical species). The reaction mechanisms are basically a combination of finite set of elementary reactions based on stoichiometric equations:

$$\sum_i \alpha_{\rho i} C_{sp_i} \rightarrow \sum_i \beta_{\rho i} C_{sp_i} \quad (1)$$

Where, $\rho = 1,\ldots,m$ are the reaction numbers and $\alpha_{\rho i}, \beta_{\rho i}$ are the stoichiometric coefficients, i. e., nonnegative integers.

The stoichiometric vectors γ_ρ of the elementary reactions are $n-$dimensional vectors with coordinates $\gamma_{\rho i} = \beta_{\rho i} - \alpha_{\rho i}$, which mean "gain minus loss" in the ρth elementary reaction.

The elementary reaction can also be written as a combination of complexes Ξ_i appears on both sides of each reaction. So, the reaction mechanism can be rewritten as a digraph of the transformation of complex $\Xi_\rho^- \mapsto \Xi_\rho^+$ i.e. vertices are complexes and edges are the reactions [8].

While a complex Ξ_i is a formal sum of $\Xi_i = \sum_{j=1}^{n} \nu_{ij} A_i$, where ν_{ij} is a vector with coordinates ν_{ij} and $\Xi_\rho^\pm$ represent the reactant and product of the reaction.

Similarly, the intermediate compounds $B_\rho^\pm$ also lie on both sides of the reactions with the complex Ξ_i thus,the above reaction mechanism (1) in extended form will take a form

$$\sum_i \alpha_{\rho i} A_i \rightleftharpoons B_\rho^- \rightarrow B_\rho^+ \rightleftharpoons \sum_i \beta_{\rho i} A_i$$

i.e., the mechanism involves two type of reactions: equilibration between a complex and its compound.

While for each nonnegative extensive variable N_i there exists an intensive variable C_i the concentration, i.e., $C_i = N_i / V$, while (volume $V > 0$). Now, the vector $C = N/V$ having coordinates c_i becomes the vector of concentrations. Similarly, the reaction rate r_ρ $(or\ w_\rho)$ is another non-negative intensive quantity, which corresponds to each reaction. The kinetic equations in the absence of external flux are:

$$\frac{dN}{dt} = V\sum_\rho \gamma_\rho r_\rho, \quad \dot{N} = VJ(c), \quad J(c) = \sum_\rho \gamma_\rho r_\rho(c) \quad (2)$$

In the case of non-constant volume, we have a different form (i.e., the case of chemical combustion) of equations for concentrations. In perfect systems and not very fast reactions, the reaction rate is a function of concentrations and temperature given by the law of mass action.

$$r_\rho(c,T) = k_\rho(T)\prod_i c_i^{\alpha\rho i} \quad (3)$$

The observed rate of reaction is the difference between the forward and backward processes $r = \vec{r} - \overleftarrow{r}$. The relation between these quantities is given by a principle of detailed balance,

$$r_\rho^+(c^{eq}) = r_\rho^-(c^{eq}) \quad (4)$$

Here $c^{eq}(T)$ represents the equilibrium for the system (2) and we consider the closed system of equations with constant volume V. For an isolated system, the extra equations are U (internal energy), V (volume) = constant, for an isochoric isothermal system, we get V, T= constant, and so forth. Therefore, (2) takes the following form in the latter case:

$$\dot{C}_{sp} = \sum_\rho \gamma_\rho r_\rho(c) = J(c) \quad (5)$$

We also consider other linear constraints in a chemical reaction, i.e., conservation of atoms takes a form:

$$D.C = B_{C_{sp}} \quad (6)$$

Where $B_{C_{sp}}$ are the balancing constants, d_i are the rows of the matrix, $D_{l\times m}$ and C involve the chemical species.

Once we are able to define the thermodynamic structure of the system, equations (2) and (6) comprise such a discrete system, in which, we are interested.

3. The Mathematical Model

Through modern model reduction techniques, a researcher can construct an invariant manifold for the system based on its initial approximation. In a dynamic system, the slow invariant manifold can be described as a slow motion along the manifold and a fast motion approaching towards them as shown in Fig. 1.

Now, let us discuss the general idea given by ILDM for the construction of invariant manifold. If the system consists of $n-$dimensional ordinary differential equations, the system will be :

$$\frac{dC}{dt} = \phi(C) \tag{7}$$

The above system describes the variation of the chemical species along with constant parameters. For the low dimension, it is important to be familiar with the time scale at each point. If there are n_s characteristic time scales (the eigenvalue of their Jacobian) then there exist n_s characteristic directions (eigenvector) associated with it. Its Jacobian J at each point in the solution space is represented as :

$$J = \begin{bmatrix} \frac{\partial \phi_1}{\partial c_1} \cdots & \cdots & \frac{\partial \phi_1}{\partial c_n} \\ \cdots & & \cdots \\ \cdots & & \cdots \\ \frac{\partial \phi_n}{\partial c_n} \cdots & \cdots & \frac{\partial \phi_n}{\partial c_n} \end{bmatrix}_0 \tag{8}$$

'0' is the point where the Jacobian is evaluated. Normally, the perturbed system can be analyzed with respect to their eigenspaces, i.e.

1. The perturbation is increasing in the direction of eigenvector in the case of positive eigen-values.
2. It shows the relaxing behavior for the negative eigen-values.
3. The zero eigen-value implies that variables are conserved at that point.

At each point, the state space of the manifold can be measured after dividing them into two subgroups, i.e., fast and slow subspace. The slow subspace arises from the fast ones n_f showing the steady state behavior towards the equilibrium and gives the value of the slow manifold $n_s = n - n_f$.

$$\{V_{c_i}, i = 1...n_f < V_{c_i}, i = n_f + 1...n\} \tag{9}$$

V_{c_i} symbolizes the fast-slow variation measured at each point. This partition reduced the possibility of solution trajectories to move along the fast direction. In this way, we are able to measure the manifold (low dimension) containing only slower time scale.

For proper removal of such possibilities of moving along the fast direction, we can take them to be in orthogonal directions. But usually, these vectors are not orthogonal. Therefore, with the help of Gram-Schmidt orthogonalization method, we apply the Schur decomposition method on Jacobian matrix, measured at each point in a phase space [11-12]. The real matrix M given by Schur decomposition is represented as:

$$M = P\mathbf{T}P^T \tag{10}$$

Here T is the transpose while T is an upper triangle having diagonal entries of eigen-values and P is an orthonormal matrix. We call P_f, P_s the transition matrices obtained from the local to the standard basis from Jacobean matrix while its inverse becomes:

$$P = (P_f, P_s), \; P^{-1} = \begin{pmatrix} \tilde{P}_f \\ \tilde{P}_s \end{pmatrix}$$

$$\begin{pmatrix} \tilde{P}_f \\ \tilde{P}_s \end{pmatrix} \left(P_f . P_s\right) = \begin{pmatrix} 1 & 0 \\ 0 & 1 \end{pmatrix} = I$$

In this way, we are able to apply the Schur decomposition method at each point of the solution space as long as the system (7) is continuous.

By definition, the ILDM can be measured from any unmeasured system of n_f equations for $n-$variables by

$$\widetilde{P_f}.\phi(C) = 0, \tag{11}$$

This vanishes the big part of the Jacobian matrix analogous to the fast time scale. Here $\widetilde{P_f}$ indicates the $(n_f \times n)$ matrix and its row partitioning is transposes of Schur matrix.

4. The Equilibrium

The equilibrium mostly deals with thermodynamics for the purpose of studying the transformations of energy and the relations between the massiveness properties of the matter. Thermodynamics is useful for model reduction in discrete systems. Although, the thermodynamics are concise by a number of laws, two of them have more significance in chemical science. The first law explains the law of conservation of energy, whereas the Second Law gives the notion of entropy and it is used to find out the direction of natural changes [13]. The importance of the Second Law of thermodynamics in chemical phenomena can be observed by the overture of the Gibbs energy of a system and the closely related chemical potential of a substance. These quantities not only allow us to monitor the natural direction of physical and chemical changes, but also the condition of chemical equilibrium when a reaction mixture has no further tendency to undergo any change.

The major idea behind this discussion is that entropy increases during the fast motion and therefore, on the plane of rapid motion, the point of entropy maximum is not very far away from the slow manifold [14]. In this region, the fast and slow motion have comparable velocities as shown in the Fig. 1.

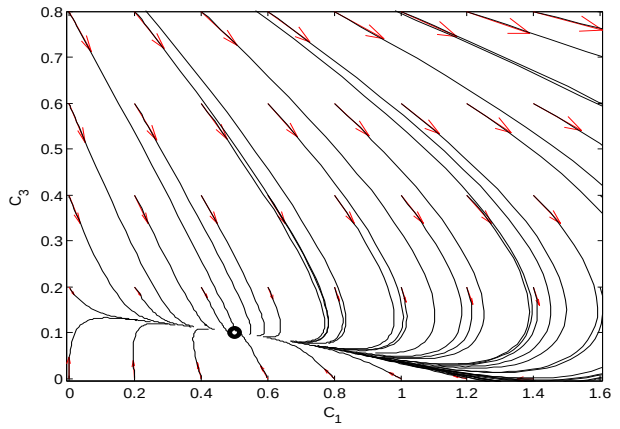

Fig 1: Fast-slow decomposition: The slow manifold passes through the equilibrium point (black circle) while the fast manifold approaches towards the equilibrium after emerging out of different points, given by [15]: $c_1 + c_3 \leftrightarrow c_4,\ c_2 + c_4 \leftrightarrow c_3 + c_5$.

5. The Scheme

In order to get all possible discrete data that lies over the manifold in the phase space, we proceed very systematically. We apply the Schur decomposition method over the Jacobian matrix, which is measured at each point other than the equilibrium point. We can deduce that it is closer to the equilibrium point and later, it moves forward to the next point $c_i^{\,g} = c_i^{\,p} + \delta c_i$ after making the correction through ILDM. The next guess point can be obtained by moving a small distance δc_i along the tangent to the manifold at that point as shown in Fig. 2.

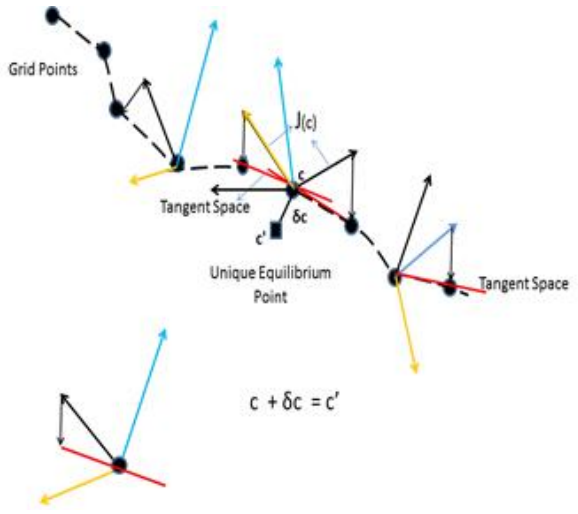

Fig 2. Shows the vector field measured at each grid point (indicated in different colors) and then it is projected (the smallest one) over the tangent space by using the Schur decomposition method.

Where pg and ng represent the previous and new guesses. Similarly, for the next points, an assumption can be made by solving this expression:

$$P^T(c_i^{\,ng} - c_i^{\,pg}) = 0 \qquad (12)$$

By knowing c^{ng}, we can further solve the above equations by using any iterative solver. The new goals can be achieved by using the previous guess. This procedure will continue until we achieve convergence within the specified tolerance. One dimensional manifold can be obtained by moving in both the directions from the equilibrium as shown in Fig. 2.

6. Refinement

The manifold obtained by an ILDM method is an initially approximated manifold. It needs to be refined by any iterative method in order to get accuracy. Therefore, a method of the invariant grid is applied here. For further details of this method, we refer the readers to [2,14,16]. The problem of the grid correction is fully decomposed into the problems of the grid's node correction, for which, we can measure a low defect of invariance at each grid point.

We use the thermodynamic projector T_p defined in [16] for our case (Eq: 5). T_p is the tangent subspace spanned by the vector e_p. Vector parallel to T_p is F and $x = (x_1, x_2, x_3)$ generate a three-dimensional vector projected onto it. We can write:

$$e_p = wf, \quad w = 1/DG(F),$$
$$Px = DG(x)e_p = (\nabla G, x)e_p,$$

While the null space of Tp has the following form:

$$(\nabla G, x) = G_1x_1 + G_2x_2 + G_3x_3 = 0,$$

And $\nabla G = (G_1, G_2, G_3)$. The dimension of $S = (\ker Tp \cap \ker B)$ is 1; whereas B is a matrix of atomic balance. Let s_1 be a vector, which spans S. Newton's [4] method of incomplete linearization is applied over each point of initially approximated SIM to refine the grid point, i.e. $(x = x_0 + \eta x : \eta x = \eta_1 s_1)$ in a form of $\eta_1 = -\dfrac{((1-Tp)J, s_1)}{((1-Tp)Ls_1, s_1)}$.

Define the concentration spaces x_i in vectorial form $M = [c_1, c_2, c_3]^T$; here, T represents a transpose. For a thermodynamic scalar product:

$$\langle x, y \rangle = (x, Hy),$$

Where (,) implies Euclidean scalar product and H is the second derivative matrix of Lyapunov function G. We define

$$J_1 = J / M, G_1 = G / M \ , \ S_1 = S / M \ , f = F / M$$

While A is a vector species.

$G(i,j) = log\left[M(i,j) - M(i,j-1) \right]$, % Gradient measure $f(i,j) = e^G / \| e^G \|$, % tangent at each point $K(i,j) = f(i,j) / (G,F)$, % Euclidean scalar product $K(i,j) = F(i,j) / (G,f)$, % Euclidean scalar product $Tp(i,j) = G_1(i,j) \times K(i,j)$, % Thermodynamic Projector $L(i,j) = \dfrac{\partial J(x)}{\partial x_i}$, % Jacobian matrix

$S_1 = null(Tp \cap B)$, % spanning set

Now, the step size is defined as

$$\eta_1 = \frac{(XJ, S_1)}{(XLb, S_1)} \ \ and \ \ X = (1 - Tp)$$

with the Euclidean scalar product. Thus

$M_1 = M + \eta_1$.

% First refinement

In the same manner, we can proceed for the second refinement if it requires

$M_2 = M_1 + \eta_2$.

% Second refinement

In our case, the second refinement remains the same.

Example

Let us implement the idea discussed above. For this, we consider an example called 'water, gas shift reaction' [17]. This system consists of two-step reversible reactions

$$\begin{aligned} C_{H_2O} + C_Z &\rightleftharpoons C_{OZ} + C_{H_2} \\ C_{OZ} + C_{CO} &\rightleftharpoons C_Z + C_{CO_2} \end{aligned} \tag{13}$$

Involving six chemical species, C_{sp}, i.e. $C_{H_2O}, C_Z, C_{OZ}, C_{H_2}, C_{CO}, C_{CO_2}$, their kinetic equation can be found through (5).

$$\frac{dC_{sp}}{dt} = \begin{bmatrix} \dot{C}_{H_2O} = k_1^- c_3 c_4 - k_1^+ c_1 c_2 \\ \dot{C}_Z \ = k_1^- c_3 c_4 - k_1^+ c_1 c_2 + k_2^+ c_3 c_5 - k_2^- c_6 c_2 \\ \dot{C}_{OZ} \ = -k_1^- c_3 c_4 + k_1^+ c_1 c_2 - k_2^+ c_3 c_5 + k_2^- c_6 c_2 \\ \dot{C}_{H_2} \ = -k_1^- c_3 c_4 + k_1^+ c_1 c_2 \\ \dot{C}_{CO} \ = -k_2^+ c_3 c_5 + k_2^- c_6 c_2 \\ \dot{C}_{CO_2} = k_2^+ c_3 c_5 - k_2^- c_6 c_2 \end{bmatrix} \tag{14}$$

The relation between molecular matrices BM and stoichiometric matrices S can easily be verified,

$$S.BM = 0 \tag{15}$$

While the balancing terms for Hydrogen, Oxygen, and Zinc are given by (7)

$$\begin{bmatrix} 2c_1 + 2c_4 \\ c_1 + c_3 + c_5 + 2c_6 \\ c_2 + c_3 \end{bmatrix} = \begin{bmatrix} b_H \\ b_O \\ b_Z \end{bmatrix} \tag{16}$$

Before applying an ILDM method (mathematical model), it is important to select the starting point to begin the process. An equilibrium point is the best option available to be considered as an initially known point on a manifold.

Let us define the following parameters

$$\begin{aligned} &c_1^{eq} = 0.5,\ c_2^{eq} = 0.1, c_3^{eq} = 0.1,\ c_4^{eq} = 0.4, \\ &c_5^{eq} = 0.1,\ c_6^{eq} = 0.1,\ k_1^+ = 1, \quad k_2^+ = 0.5 \end{aligned} \tag{17}$$

Now, we are interested in the reduced form of the system (13) with the help of (16) in order to measure the variation of the variables with respect to fast and slow variables. Therefore, the Jacobian measured at an equilibrium point gives the following outcome:

$$L = \partial J / \partial c_i \ = \begin{bmatrix} -0.2250 & 1.0000 & 0.0000 \\ 0.2750 & -1.0500 & 0.1500 \\ -0.0500 & 0.0500 & -0.1500 \end{bmatrix} \tag{18}$$

Moving towards the next guess point c^g near the equilibrium point c^{eq} in a forward (backward) direction we have an equation:

$$r = c^{eq} \pm h \times b \tag{19}$$

Whereas h is the step size and b is the slowest eigenvector corresponding to the lowest eigenvalue. The eigenspace span by the system is carefully planned at each defined time interval. By implementing model reduction and using the Schur decomposition at each point, it may be possible to get its analytical solutions or

even by hand calculation might be valid to some extent, but for a large system,(just like the one we have)it is preferable to make its numerical calculations.

Now, the transition matrix (18) is given by

$$Q = \begin{bmatrix} 0.1786 & 0.2449 & 0.9529 \\ 0.6734 & -0.7365 & 0.0631 \end{bmatrix} \tag{20}$$

While the variation observed here is as follows:

$$V_{c1} < V_{c6} < V_{c3} \tag{21}$$

Now, in the reduced form of the system, it no longer remains stiff and it is feasible to get the whole solution of the system. Similarly, moving in both forward and backward directions from the equilibrium position, their increasing, and decreasing order can easily be measured as depicted in Fig. 3. Now, it is important to mention here that the points on the manifolds represent an intrinsic low-dimensional attractive manifold and they are well described by the slow time scale after decaying the fast time scales.

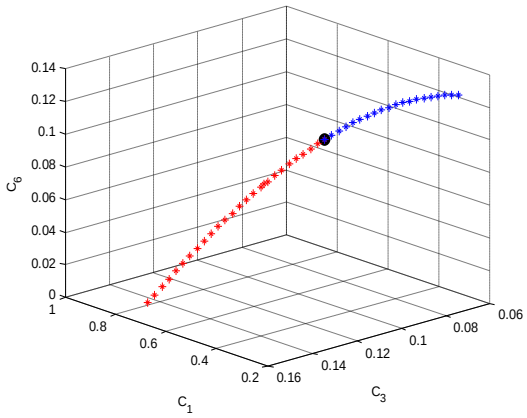

Fig 3: 1D ILDM measured in 3D. Starting from an equilibrium point (black circle), it first moved to its forward direction (blue line) and then in backward direction (red line) with h=0.01

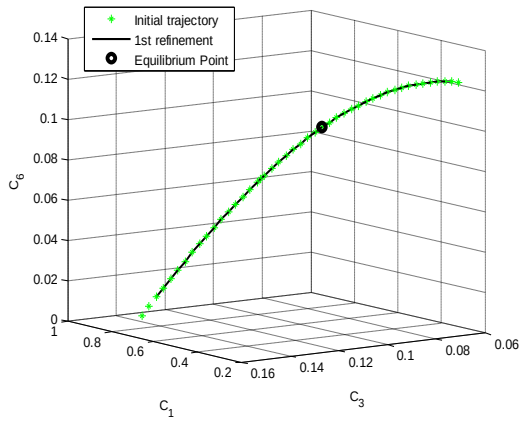

Fig 4: 1D ILDM measured in 3D is further refined with the method of invariant grids and no change was observed during the process.

According to the first refinement carried out with the MIG in Fig. 4, there is no change in the solution curve. Therefore, we extended our efforts towards the higher dimension and obtained the 2D curves in three dimensions by keeping h=0.01 using the fact that one dimension ILDM belongs to two-dimensional ILDMs and so on. This idea can be used to compute the ILDM of the second order and to do that, we must divide the one-dimensional ILDM into small intervals at each point of that subdivision advanced in both directions following the procedure outlined in Fig. 5.

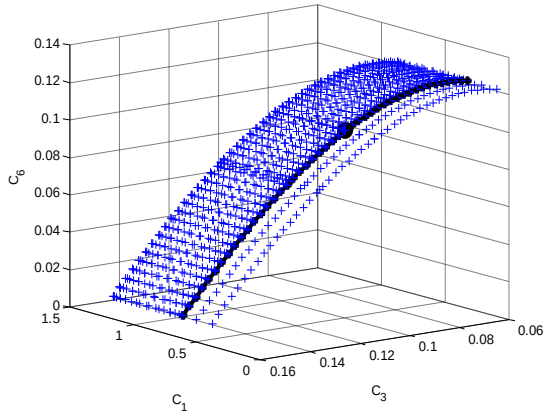

Fig 5: 2D ILDM measured in 3D with h=0.01. Black circle lines indicate the 1D ILDM lies in the 2D blue star lines.

6. Conclusion

In order to be aware of the chemical changes occurred during the molecular mechanism, we need to understand how molecules behave during the reactions. They either move through free flight gasses or by diffusion through liquids. The present paper is also concerned with changes in the chemical species and we precisely studied their rates of chemical reactions.

Specifically, in the case of complex chemical kinetics with a known detailed narration of the system, we usually solve the initial value problem for the system. But we fail when we have information about only a small part of the interacting system.

The graphic representation of the chemical species and their variation with respect to time clears the idea of fast and slow trajectories. Through proper algorithm and grid size variations, we started measuring an equilibrium point. The idea is then extended to an approximated 1D ILDM solution, which is then refined with the method of invariant grids. Similarly, the formulations for the higher-dimension manifolds are discussed and involved a larger number of time scales, which simply means that more progress variables were added to the manifold for the construction.

References

[1] A.N. Gorban, I.V. Karlin, "Method of invariant manifold for chemical kinetics", Chemical Engineering Science, vol. 58, pp. 4751-4768, 2003.

[2] A.N. Gorban, I.V. Karlin, A.Y. Zinovyev, "Invariant grids for reaction kinetics", Physica A: Statistical Mechanics and its Applications, vol. 333, pp. 106-154, 2004.

[3] U. Maas, S.B. Pope, "Simplifying chemical kinetics: intrinsic low-dimensional manifolds in composition space", Combustion and Flame, vol. 88, pp. 239-264, 1992.

[4] V. Bykov, I. Goldfarb, V. Gol'Dshtein, U. Maas, "On a modified version of ILDM approach: asymptotic analysis based on integral manifolds", IMA J.Appl.Maths., vol. 71, pp. 359-382, 2006.

[5] E. Chiavazzo, I.V. Karlin, "Quasi-equilibrium grid algorithm: Geometric construction for model reduction", J. Comput. Phys., vol. 227, pp. 5535-5560, 2008.

[6] M. Shahzad, H. Arif, M. Gulistan, M. Sajid, "Initially approximated quasi equilibriummanifold", J. Chem. Soc. of Pakistan, vol. 37, pp. 207-216, 2015.

[7] A.S.A.Khan, Equilibrium and Thermodynamic Study of Cadmium Adsorption on Dalbergia Sissoo Sawdust, The Nucleus, vol. 53, no. 1, pp. 1-8, 2016.

[8] J. Warnatz, U. Maas, "Calculation of the detailed structure of premixed and non-premixed flame fronts and some applications, Proc. 12th IMACS World Congress, vol. 3, p. 614, 1989.

[9] G. Stahl, J. Warnatz, "Numerical investigation of time-dependent properties and extinction of strained methane瑿 and propane-air flamelets", Combustion and Flame, vol. 85, pp. 285-299, 1991.

[10] R.J. Kee, J.A. Miller, G.H. Evans, G. Dixon-Lewis, A computational model of the structure and extinction of strained, opposed flow, premixed methane-air flames, in: Symposium (International) on Combustion, Elsevier, pp. 1479-1494, 1989.

[11] G.H. Golub, C.F. Van Loan, Matrix computations. Johns Hopkins series in the mathematical sciences, Johns Hopkins University Press, Baltimore, MD, 1989.

[12] W.W. Hager, Applied numerical linear algebra, Prentice Hall, 1988.

[13] A.N. Gorban, M. Shahzad, The michaelis-menten-stueckelberg theorem, Entropy, vol. 13, pp. 966-1019, 2011.

[14] A.N. Gorban and I.V. Karlin, "Thermodynamic parameterization", Physica A: Statistical Mechanics and its Applications, vol. 190, pp. 393-404, 1992.

[15] M. Shahzad, S. Rehman, R. Bibi, H.A. Wahab, S. Abdullah, S. Ahmed, "Measuring the complex behavior of the SO2 oxidation reaction", Computational Ecology and Software, vol. 5, pp. 254-270, 2015.

[16] A.N. Gorban, I.V. Karlin, Invariant Manifolds for Physical and Chemical Kinetics, vol. 660 of Lect. Notes Phys. Springer, Berlin Heidelberg. 2005.

[17] G. Marin, G.S. Yablonsky, "Kinetics of chemical reactions", John Wiley & Sons, 2011.